Hydrogen-Bonded Structure in Concentrated Aqueous Phosphoric Acid Solutions

Yasuo Kameda,* Kentaro Sugawara, Takayoshi Hosaka, Takeshi Usuki, and Osamu Uemura

Department of Material and Biological Chemistry, Faculty of Science, Yamagata University, Kojirakawa-machi 1-4-12, Yamagata 990-8560

(Received November 12, 1999)

Polarized Raman scattering, X-ray, and time-of-flight (TOF) neutron-diffraction measurements were carried out for highly concentrated aqueous phosphoric acid solutions, in order to deduce detailed structural information on both the PO_4-intramolecular geometry and intermolecular hydrogen bonds in the solution. Isotropic Raman spectra observed for $(H_3PO_4)_x(H_2O)_{1-x}$ with x = 0.1—0.6 exhibited a single band assigned to the symmetrical stretching vibrational mode of the PO_4 structural unit, which suggests that all P–O bonds in the unit are spectroscopically equivalent. The results of X-ray and neutron-diffraction measurements for the 53 mol% phosphoric acid solution indicated that the structure of the PO_4 unit is a regular tetrahedron with a P–O bond-length of 1.540(3) Å. From a least-squares fit to the observed X-ray and neutron intermolecular interference terms, the nearest-neighbor intermolecular distances, reflecting intermolecular hydrogen-bonded interactions in the solution, were determined to be r(O···D) = 1.77(1) Å and r(O···O) = 2.73(2) Å, respectively, which are both ca. 0.1 Å shorter than those observed for pure liquid water. Therefore, it has been clarified that a strongly hydrogen-bonded network exists in such concentrated aqueous phosphoric acid solutions.

Phosphoric acid is one of the most important compounds over the extensive field of industrial, inorganic and biological chemistry. The geometry of H_3PO_4 molecules in crystalline phosphoric acid has been known to be a distorted tetrahedron with three longer P–O(H) bonds (1.568—1.577 Å,[1] 1.547—1.563 Å [2]), and one shorter P=O one (1.517 Å,[1] 1.494—1502 Å [2]), respectively. A significant difference between the P–O(H) (1.542—1.561 Å) and P=O (1.477—1.503 Å) bond distances has also been reported in crystalline hydrate, $H_3PO_4 \cdot 1/2H_2O$.[3] On the other hand, a recent neutron-diffraction study has revealed that intramolecular P–O bonds in pure liquid phosphoric acid have a symmetrical distribution centered at r = 1.54(1)Å, [4] corresponding to the regular tetrahedral geometry of the PO_4 structural unit in the liquid state. According to an X-ray diffraction study by Caminiti et al., the average P–O distance has been observed to be 1.60 Å in an aqueous 3.84 mol% H_3PO_4 solution and 1.55 Å in a 11.47 mol% H_3PO_4 solution, respectively.[5] These values were derived from the intramolecular O···O distance within the PO_4 unit employing a least-squares fitting analysis on the basis of the regular tetrahedral geometry of this unit. More direct information on the geometry of the PO_4 unit in aqueous phosphoric acid solutions can be provided by a least-squares fitting analysis to the observed X-ray and neutron interference terms in a sufficiently high-Q region. Regarding the fitting procedure, a more detailed structural model for chemically dominant species, H_3PO_4 and $H_2PO_4^-$, should be adopted, in which the intramolecular P=O and P–O(H) bond-lengths are allowed to vary independently.

Studies on the intermolecular hydrogen-bonded structure in aqueous acidic solutions have long been a matter of interest, in connection with the fast proton transfer phenomena, which play an important role in chemical and biological processes in aqueous solution. Earlier X-ray diffraction studies for concentrated aqueous HCl solutions have indicated that the hydrogen-bonded network structure in the aqueous acidic solution is characterized by a very short intermolecular O···O distance (2.56 Å, [6] 2.5—2.6 Å, [7] 2.44(1) Å, [8] and 2.52(2) Å [9]) between H_3O^+ and the nearest-neighbor H_2O molecules. However, it has generally been difficult to obtain corrected information concerning the distribution of hydrogen atoms in the aqueous solution from X-ray diffraction data alone. A neutron-diffraction measurement may be considered to be more suitable, because the positions of the hydrogen atoms in the hydrogen-bonded network structure can be specified. Triolo and Narten have carried out X-ray and neutron-diffraction measurements for aqueous HCl and DCl solutions over an extended concentration range.[9] They have reported a very short intermolecular hydrogen-bonded O···D distance, 1.61(2) Å, between D_3O^+ and the nearest-neighbor D_2O molecules, which corresponds well to the shorter O···O distance given in earlier X-ray diffraction studies. This short O···D distance has been confirmed by a recent neutron diffraction measurement for an aqueous 21 mol% HCl solution by the authors,[10] in which the H/D isotopic substitution technique was applied to obtain partial structure factors, $a_{HH}(Q)$, $a_{XH}(Q)$, and $a_{XX}(Q)$, (X: O, Cl) separately. The authors have obtained the nearest-neighbor O···H(D) distance, 1.69(2) Å, by a least-squares fitting analysis to the observed $a_{XH}(Q)$. Recently, the authors have estimated highly resolved X-ray and neutron distribution functions in an aqueous sulfuric acid solution,[11] and obtained con-

siderably short intermolecular hydrogen-bonded distances of $r(O\cdots D) = 1.7$ Å and $r(O\cdots O) = 2.7$ Å, which implies the presence of the hydrogen bonds between the sulfuric acid and the nearest-neighbor water molecules. In this work, it has also been confirmed that the hydrogen bonds among sulfuric acid molecules are more strongly formed than in the case among water molecules in pure liquid water. Moreover, Andreani et al. have investigated intermolecular hydrogen-bonded correlations in concentrated aqueous sulfuric acid solutions by combining X-ray and neutron-diffraction data.[12,13] Therefore, it seems of considerable interest to investigate the hydrogen-bonded network structure in much weaker oxoacid solutions, in which both hydrogen bonds between the oxoacid molecule and the nearest-neighbor H_2O molecules, as well as those among oxoacid molecules, should play an important role concerning the physical and chemical properties of the solution.

In the present paper we describe the results of X-ray and neutron diffraction measurements for highly concentrated aqueous 53 mol% phosphoric acid solutions to investigate both the intramolecular geometry within the H_3PO_4 molecule and the intermolecular hydrogen-bonded network structure in the solution. In addition, the concentration dependence of the symmetrical stretching vibrational band of the PO_4 unit in the aqueous phosphoric acid solution has been investigated by means of the isotropic Raman spectroscopy.

Experimental

Raman Scattering Measurements. Aqueous phosphoric acid solutions, $(H_3PO_4)_x(H_2O)_{1-x}$ with x = 0.1, 0.2, 0.3, 0.4, 0.5, and 0.6, respectively, were prepared by dissolving weighted amounts of crystalline anhydrous H_3PO_4 (Merck, Guaranteed grade) into distilled H_2O. The composition of the solution was checked by the standard acid-base titration. All of the sample solutions were filtered through a 0.45 μm Teflon® millipore filter to remove any dust particle before introducing them into a Pyrex® Raman cell (10×10 mm and 40 mm H). Polarized Raman spectra were recorded at 25 °C in the frequency range of $800 \leq \nu \leq 1000$ cm^{-1} using a JASCO NR-1100 spectrometer with a 514.5 nm line of NEC GLG-3200 Ar^+ laser operated at 100 mW. The calibration of the monochromator was made using 89 neon emission lines. The efficiency of the polarization filter was carefully checked through a measurement of the depolarization ratio of the ν_1, ν_2, and ν_4 bands of the CCl_4 molecule in the liquid state. Details of the Raman scattering measurement are all identical to those described in our previous papers.[14,15]

X-Ray Diffraction Measurement. X-ray diffraction intensities with the Mo$K\alpha$ radiation (λ = 0.7107 Å) were measured at 25 °C for an aqueous 53 mol% H_3PO_4 solution under the reflection geometry using a θ–θ X-ray diffractometer manufactured by Rigaku Co. Scattered X-ray intensities were collected at an interval of 0.2° over the angular range $3 \leq 2\theta \leq 150°$, corresponding to that of the scattering vector magnitude, $0.5 \leq Q \leq 17.1$ Å^{-1} ($Q = 4\pi\sin\theta/\lambda$), with a fixed counting time of 100 s. The whole angular range in each measurement was scanned three times to maintain good statistics of the diffraction data, and to minimize any long-term instrumental drift. The total number of counts per one data-point reached at least 2.9×10^5. Details of the X-ray diffraction measurement have already been described elsewhere.[16]

Neutron Diffraction Measurement. A fully deuterated 53 mol% D_3PO_4–D_2O solution (99% D, Aldrich Chemical Co.) was sealed into a cylindrical quartz cell with 7.3 mm in inner diameter and 0.5 mm in thickness. A TOF neutron diffraction measurement was carried out at 25 °C using the HIT-II spectrometer[17] installed at the pulsed spallation neutron source (KENS) at the High Energy Acceleration Research Organization (KEK), Tsukuba, Japan. The data-acquisition time in the present measurement was 6.5 h. Measurements for an empty cell, a vanadium rod with the same dimension as that of the sample and background, were made in advance.

Data Reduction

Raman Scattering Data. The isotropic Raman intensity ($I^{iso}(\nu)$) after a correction for the Bose–Einstein factor,[18–21] can be obtained by

$$I^{iso}(\nu) = I^{//}(\nu) - 4/3\cdot I^{\perp}(\nu), \tag{1}$$

where $I^{//}(\nu)$ and $I^{\perp}(\nu)$ denote the corrected parallel and perpendicular spectra, respectively. The phosphorescence background, which is often unavoidable for a sample containing P atoms, is preferably eliminated in the isotropic spectrum. Since vibrational modes with a higher symmetry in the solution should appear in the isotropic spectrum, band components in the spectrum will be simply interpreted.

X-Ray Diffraction Data. The correction and normalization procedures for the observed X-ray intensities were almost similar to those described in our previous paper.[16] The observed total X-ray interference term ($i_X(Q)$) is given as

$$i_X(Q) = (I_{eu}(Q) - \langle f^2\rangle)/\langle f\rangle^2, \tag{2}$$

where

$$\langle f^2\rangle = \sum c_i[(f_i(Q)+f_i')^2 + f_i''^2] \tag{3}$$

and

$$\langle f\rangle^2 = \left[\sum c_i(f_i(Q)+f_i')\right]^2 + \left[\sum c_i f_i''\right]^2, \tag{4}$$

respectively. $I_{eu}(Q)$ expresses the normalized coherent scattering intensity in the electron unit, and $f_i(Q)$ corresponds to the atomic scattering factor of atom i. The real and imaginary parts for the anomalous dispersion factor are denoted by f_i' and f_i'', respectively. The X-ray distribution function ($g_X(r)$) can be evaluated by a Fourier transform of $i_X(Q)$ with the upper limit of the integral, Q_{max} = 17.1 Å^{-1};

$$g_X(r) = 1 + (2\pi^2\rho r)^{-1}\int_0^{Q_{max}} Q i_X(Q)\sin(Qr)\mathrm{d}Q. \tag{5}$$

$i_X(Q)$, scaled by the stoichiometric unit, $(H_3PO_4)_x(H_2O)_{1-x}$, is the sum of intra- and intermolecular interference terms,

$$i_X(Q) = i_X^{intra}(Q) + i_X^{inter}(Q), \tag{6}$$

where

$$i_X^{intra}(Q) = (x-y)\cdot i_X^{intra}(Q)\ (\text{for } H_3PO_4) + y\cdot i_X^{intra}(Q)\ (\text{for } H_2PO_4^-) + y\cdot i_X^{intra}(Q)\ (\text{for } H_3O^+) + (1-x-y)\cdot i_X^{intra}(Q)\ (\text{for } H_2O). \tag{7}$$

The value of y when x = 0.53 can approximately be evaluated to be 0.0236 from the acid dissociation constant for H_3PO_4,[22]

indicating that 96% of the phosphoric acid molecule exists in the H_3PO_4 form. Contributions from highly dissociated species, HPO_4^{2-} and PO_4^{3-}, are neglected because of the small contribution to the total interference term. The intramolecular interference term for each chemical species in Eq. 7 can be estimated through the Debye's equation,

$$i_X^{intra}(Q) = \sum_{i \neq j} \sum [(f_i(Q) + f_i')(f_j(Q) + f_j') + f_i'' f_j''] \times \exp(-l_{ij}^2 Q^2/2) \sin(Qr_{ij})/(Qr_{ij})/\langle f \rangle^2, \quad (8)$$

where, l_{ij} and r_{ij} denote the root-mean-square displacement and interatomic distance for i–j pair, respectively. The least squares fit to the observed total interference term was performed in the range of $9.0 \leq Q \leq 17.1$ Å^{-1} using the SALS program.[23] The following assumptions were made for setting up the calculated intramolecular interference term: (a) The intramolecular O–H and H–H distances, r_{OH} and r_{HH}, within H_2O and H_3O^+ molecules and their r.m.s. displacements, l_{OH} and l_{HH}, are fixed at values reported in our previous TOF neutron diffraction study.[24] (b) The intramolecular P=O and P–O(H) distances, their r.m.s. displacements, and the bond angle ∠ O=P–O(H) were allowed to vary independently in the preliminary analysis, but even if different initial values such as r(P=O) = 1.50 Å and r(P–O(H)) = 1.55 Å, were adopted in the least squares calculation, both values were finally converged around 1.54 Å, in other words, it appears that all P–O bonds have the same distance in the aqueous 53 mol% phosphoric acid solution. Consequently, we can assume the tetrahedral geometry for the PO_4 unit. The P–O distance and its r.m.s. displacement, and the r.m.s. displacement for the O···O interaction within the PO_4 unit were treated as independent parameters in the present fitting procedure.

The observed X-ray intermolecular interference term was derived by subtracting the calculated intramolecular contribution from the observed total interference term. The calculated intermolecular interference term, $i_X^{calc}(Q)$, was set up by summing the nearest-neighbor short-range interaction term, $i_X^s(Q)$, and the long-range one for all possible atom pairs in the solution, $i_X^l(Q)$,

$$i_X^{calc}(Q) = i_X^s(Q) + i_X^l(Q), \quad (9)$$

where

$$i_X^s(Q) = \sum i_{X_{ij}}(Q) \quad (10)$$

and

$$i_{X_{ij}}(Q) = (2 - \delta_{ij}) c_i n_{ij} [(f_i(Q) + f_i')(f_j(Q) + f_j') + f_i'' f_j''] \times \exp(-l_{ij}^2 Q^2/2) \sin(Qr_{ij})/(Qr_{ij})/\langle f \rangle^2. \quad \begin{cases} \delta_{ij} = 1 \ (i = j) \\ \delta_{ij} = 0 \ (i \neq j). \end{cases} \quad (11)$$

The long-range interaction term was given using the following equation:[25–27]

$$i_X^l(Q) = 4\pi\rho \sum c_i c_j [(f_i(Q) + f_i')(f_j(Q) + f_j') + f_i'' f_j''] \times \exp(-l_{0ij}^2 Q^2/2)[Qr_{0ij} \cos(Qr_{0ij}) - \sin(Qr_{0ij})] Q^{-3}, \quad (12)$$

where, r_{0ij} denotes the distance beyond which a continuous distribution of atom j around atom i is assumed. The parameter l_{0ij} describes the sharpness of the boundary at r_{0ij}. Parameters n_{ij}, l_{ij}, and r_{ij}, in Eq. 11, and l_{0ij} and r_{0ij} in Eq. 12 were, respectively, determined by a least-squares fit of Eq. 9 to the observed $i_X^{inter}(Q)$. The present fitting procedure was performed in the range $1.0 \leq Q \leq 15.0$ Å^{-1} using the SALS program.[23] In the procedure, values of l_{0ij} and r_{0ij} in $i_X^l(Q)$ were respectively assumed to have the same value for all i–j pairs because of the reduction of the number of independent parameters.

Neutron Diffraction Data. The observed scattering intensities were corrected for background, absorption,[28] and multiple[29] and incoherent scattering. The corrected intensities were converted to the absolute scale using the corrected scattering intensities from the vanadium rod. Scattering data from 64 sets of lower scattering angle detectors located at $10 \leq 2\theta \leq 51°$ were combined so as to minimize the inelasticity distortion of the observed cross section, were then employed for a subsequent analysis. A correction for low-frequency systematic errors was made in the same manner as that indicated in a previous paper.[24]

The observed neutron total interference term, scaled by the stoichiometric unit, $(D_3PO_4)_x(D_2O)_{1-x}$, is divided into intra- and intermolecular interference terms:

$$i_N(Q) = i_N^{intra}(Q) + i_N^{inter}(Q), \quad (13)$$

where

$$i_N^{intra}(Q) = (x - y) \cdot i_N^{intra}(Q) \text{ (for } D_3PO_4) + y \cdot i_N^{intra}(Q) \text{ (for } D_2PO_4^-) + y \cdot i_N^{intra}(Q) \text{ (for } D_3O^+) + (1 - x - y) \cdot i_N^{intra}(Q) \text{ (for } D_2O). \quad (14)$$

The neutron intramolecular interference terms for D_3PO_4, $D_2PO_4^-$, D_3O^+, and D_2O, respectively, are obtained from Eq. 8 by replacing the atomic scattering factor for X-rays ($f_i(Q)$) by the coherent neutron scattering length (b_i). A least-squares fit to the observed $i_N(Q)$ was applied in the range of $12.0 \leq Q \leq 40.0$ Å^{-1} using Eq. 14. In the fitting procedure, the structural parameters for D_3O^+ and D_2O molecules were referred to those obtained in our previous paper.[24] The tetrahedral geometry of the PO_4 unit was assumed as mentioned in the above section. The parameters, r(P–O), l(P–O), and l(O···O), respectively, were allowed to vary independently. Contributions from the intramolecular O–D and P···D correlations within the D_3PO_4 and $D_2PO_4^-$ molecules were added in the calculated $i_N^{intra}(Q)$ because of the relatively large value of b_D. Structural parameters, r(O–D), l(O–D), l(P···D), and ∠P–O–D, respectively, were treated as independent parameters. The observed $i_N^{inter}(Q)$ was derived by subtracting the calculated $i_N^{intra}(Q)$ from the observed $i_N(Q)$. The calculated $i_N^{inter}(Q)$ is given by Eqs. 9, 10, 11, and 12 by replacing $f_i(Q)$ by b_i. A least-squares fit to the observed $i_N^{inter}(Q)$ was carried out in the $1.0 \leq Q \leq 15.0$ Å^{-1} range using the SALS program.[23] In the fitting procedure, short-range structural parameters (r_{ij}, l_{ij}, and n_{ij}) and long-range ones (r_{0ij} and l_{0ij}) respectively, were allowed to vary independently. The neutron distribution function, $g_N(r)$, was obtained by the Fourier

transform of $i_N(Q)$ by the following equation:

$$g_N(r) = 1 + (2\pi^2\rho r)^{-1}(\sum c_i b_i)^{-2} \int_0^{Q_{max}} Q i_N(Q) \sin(Qr) dQ. \quad (15)$$

The upper limits of the integral, $Q_{max} = 40.0$ and 17.1 Å^{-1}, respectively, were adopted for the total- and intermolecular distribution functions.

Results and Discussion

The observed isotropic Raman spectra in $(H_3PO_4)_x(H_2O)_{1-x}$ solutions with $x = 0.1$—0.6 are shown in Fig. 1, in which vibrational modes with the higher symmetry should be involved. The polarized peak at ca. 900 cm^{-1} is attributed to the symmetrical stretching vibrational mode of the PO_4 unit. Although the position of the peak slightly shifts toward the higher frequency side with increasing x, only a single peak is observed at all x. If P=O and P–O(H) bonds with different bond-lengths were present in these solutions, two independent peaks corresponding to these bonds should appear, possibly at around 865 cm^{-1} (P–O(H)) and 976 cm^{-1} (P=O) as has been observed in an aqueous K_2HPO_4 solution.[30,31] Therefore, the present Raman result implies that all P–O bonds are spectroscopically identical in concentrated aqueous H_3PO_4 solutions, which is in contrast to that in the concentrated aqueous sulfuric acid solution in which various S–O stretching vibrational bands separately appear.[32]

The observed $i_X(Q)$ and the corresponding $g_X(r)$ in the aqueous 53 mol% H_3PO_4 solution are represented in Figs. 2 and 3, respectively. The dominant first peak at $r \approx 1.5$ Å in $g_X(r)$ is assigned to the intramolecular P–O interactions. The second peak at $r \approx 2.5$ Å is attributable to the intramolecular O···O interactions within the tetrahedral PO_4 unit. Structural parameters, r_{PO}, l_{PO}, and l_{OO}, respectively, within the PO_4 unit are determined by a least-squares fit of the calculated $i_N^{intra}(Q)$ (Eq. 7) to the observed $i_X(Q)$ in the range $9.0 \leq Q \leq 17.1$ Å^{-1}, where intermolecular interference contributions can be regarded to dump out. The fitting result

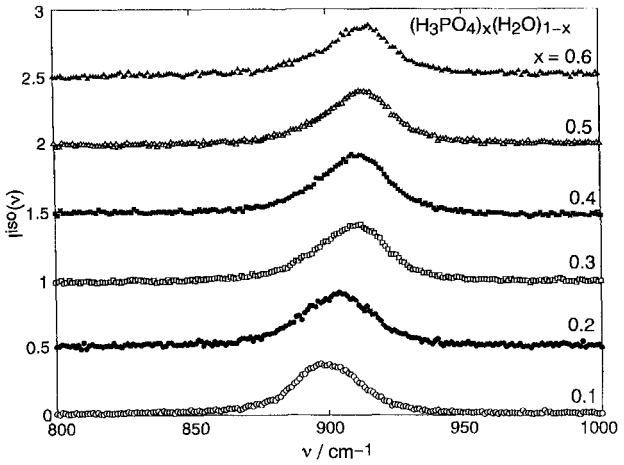

Fig. 1. Observed isotropic Raman spectra in the P–O stretching region for $(H_3PO_4)_x(H_2O)_{1-x}$, $x = 0.1$, 0.2,0.3, 0.4, 0.5, and 0.6.

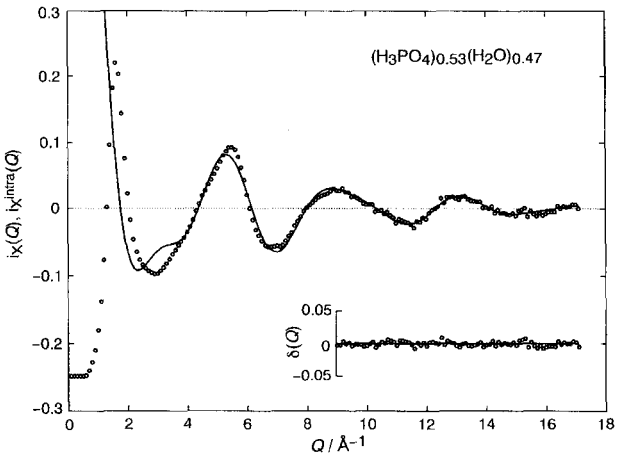

Fig. 2. Observed X-ray total interference term, $i_X(Q)$, for aqueous 53 mol% H_3PO_4 solution (circles) and the best-fit results for intramolecular contribution (solid line). Residual functions are given below (circles).

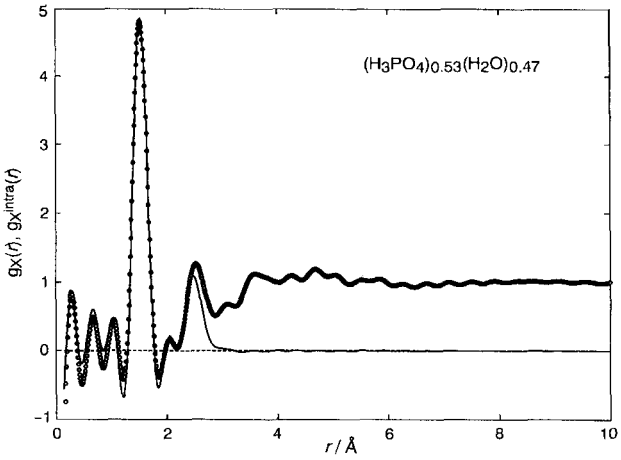

Fig. 3. Observed X-ray total distribution function, $g_X(r)$, for aqueous 53 mol% H_3PO_4 solution (circles) and the Fourier transform of the calculated intramolecular interference term (solid line).

is summarized in Table 1. The present value of the P–O distance (1.539(2) Å) is in complete agreement with that reported in pure liquid phosphoric acid (r_{PO} = 1.54(1) Å),[4] and also agrees well with the average of the shorter P=O and longer P–O(H) distances, r_{PO} = 1.544 Å, in a single-crystal of

Table 1. Intramolecular Parameters for H_3PO_4 (D_3PO_4) Unit in Aqueous 53 mol% H_3PO_4 (D_3PO_4) Solutions[a)]

	Neutron $12 \leq Q \leq 40$ Å^{-1}	X-ray $9 \leq Q \leq 17$ Å^{-1}
r(P–O)/Å	1.5396(6)	1.539(2)
l(P–O)/Å	0.0573(2)	0.099(2)
l(O···O)/Å	0.1029(5)	0.120(3)
r(O–D)/Å	0.9769(6)	—
l(O–D)/Å	0.1036(3)	—
l(P···D)/Å	0.0908(7)	—
∠P–O–D/°	113.0(1)	—

a) Estimated standard deviations are given in parentheses.

anhydrous phosphoric acid.[2] Further, the value is very close to r_{PO} = 1.548 Å observed in phosphoric acid hemihydrate.[3]

The observed $i_N(Q)$ and the corresponding $g_N(r)$ in an aqueous 53 mol% D_3PO_4 solution in D_2O are given in Figs. 4 and 5, respectively. The first peak at $r \approx 1$ Å in $g_N(r)$ is assigned to the intramolecular O–D interactions within D_2O, D_3O^+, D_3PO_4, and $D_2PO_4^-$ molecules, respectively. The second peak at $r \approx 1.5$ Å is attributable to the sum of contributions from the intramolecular P–O correlations within the PO_4 unit and from intramolecular non-bonding D···D interactions within D_2O and D_3O^+ molecules, respectively. The O···O interactions within the PO_4 unit are observable as the third peak of $g_N(r)$ at $r \approx 2.5$ Å. The partially resolved hump at $r \approx 2.1$ Å may be attributable to the intramolecular P···D interactions within D_3PO_4 and $D_2PO_4^-$ molecules, respectively. Structural parameters for these molecules can be obtained by a least-squares fit of the calculated $i_N^{intra}(Q)$ (Eq. 14) to the observed $i_N(Q)$ in the range of $12.0 \leq Q \leq 40.0$ Å^{-1}, under the assumption that statistical errors uniformly distribute in this Q range. The fitting results are summarized also in Table 1. The P–O distance obtained from the neutron diffraction data is in complete agreement with that from the X-ray ones. However, the value of l(P–O) from the neutron data is somewhat smaller than that from the X-ray ones. This discrepancy may be explained by the difference of the Q-range covered in the least-squares fit between both data, because the amplitude of the P–O intramolecular interference term has larger values beyond the higher-Q region than that of the O···O one owing to smaller values of both the interatomic distance and the r.m.s. amplitude. The value of l(P–O) obtained from the neutron data is therefore considered to be more reliable than that from X-ray data with the limited Q-range. Although the present values of the intramolecular O–D distance within D_3PO_4 and $D_2PO_4^-$ molecules are similar to that observed for liquid pure D_2O, the relatively large l(O–D) obtained for D_3PO_4 (and for $D_2PO_4^-$) indicates that a considerable fluctuation of the O–D distance occurs in a concentrated aqueous phosphoric acid solution. The bond angle of ∠P–O–D is determined to be 113.0(1)° in the present work.

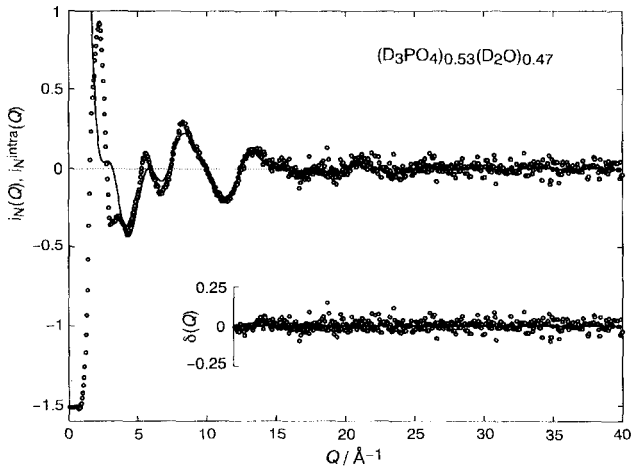

Fig. 4. Observed neutron total interference term, $i_N(Q)$, for aqueous 53 mol% D_3PO_4 solution in D_2O (circles) and the best-fit results for intramolecular contribution (solid line). Residual functions are given below (circles).

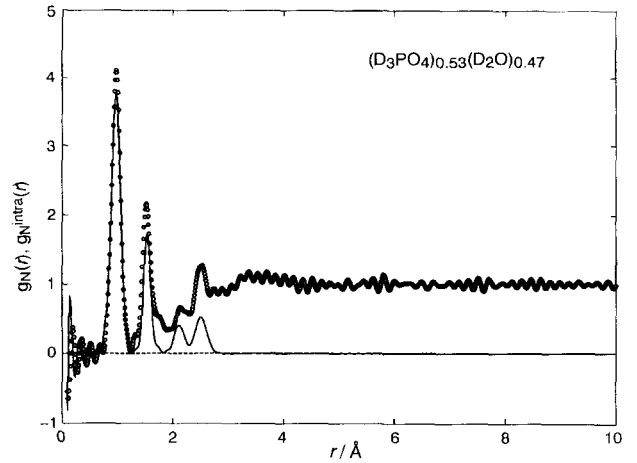

Fig. 5. Observed neutron total distribution function, $g_N(r)$, for aqueous 53 mol% D_3PO_4 solution in D_2O (circle) and the Fourier transform of the calculated intramolecular interference term (solid line).

The intermolecular distribution functions, $g_N^{inter}(r)$ and $g_X^{inter}(r)$, (Fig. 6) were respectively derived by the Fourier transform of the observed intermolecular interference terms, $i_N^{inter}(Q)$ and $i_X^{inter}(Q)$, obtained by subtracting the calculated intramolecular interference term from the observed total interference term. The neutron intermolecular distribution function, $g_N^{inter}(r)$, is characterized by the well-defined first peak at $r \approx 1.8$ Å, attributed to nearest neighbor hydrogen-bonded O···D interactions in the solution. Further, the partially resolved peak at $r \approx 3.6$ Å and a shoulder at $r \approx 2.7$ Å are observed in $g_X^{inter}(r)$. The difference of the observed $g_N^{inter}(r)$ and $g_X^{inter}(r)$ reflects that of the scattering amplitude of constituent atoms against incident neutron and X-ray radiations. The observed $g^{inter}(r)$ is given by the weighted sum of six partial distribution functions. The relative weightings of the partial distribution functions observed for neutron and X-ray diffraction data are indicated in Table 2. However, the contribution from at least one atomic pair can be canceled out by taking the difference between the observed $g_N^{inter}(r)$ and $g_X^{inter}(r)$. In order to delete the O–O contribution, we can

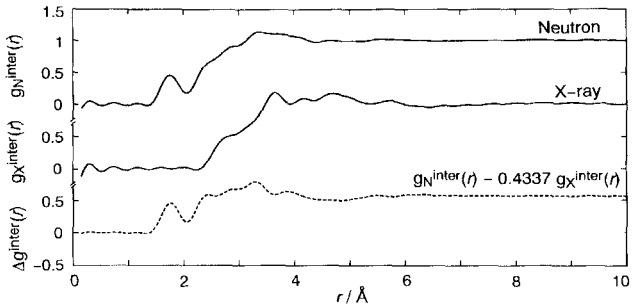

Fig. 6. Neutron and X-ray intermolecular distribution functions (solid lines). Difference distribution function, $\Delta g^{inter}(r)$, in which contribution from O–O pair has been deleted, is shown by a broken line.

Table 2. Relative Weightings of Partial Distribution Functions for Neutron and X-Ray Total $g_N(r)$, $g_X(r)$ Functions, and for the Difference Distribution Function, $\Delta g(r)$ ($=g_N(r) - 0.4337g_X(r)$), Respectively

i–j	P–P	P–O	P–H	O–O	O–H	H–H
$g_N(r)$	0.006	0.069	0.076	0.191	0.423	0.235
$g_X(r)$	0.065	0.338	0.041	0.441	0.108	0.007
$\Delta g(r)$	−0.022	−0.078	0.058	0	0.376	0.232

choose 0.4337 as a coefficient for $g_X^{inter}(r)$,

$$\Delta g^{inter}(r) = g_N^{inter}(r) - 0.4337 g_X^{inter}(r). \quad (16)$$

Since $\Delta g^{inter}(r)$ is mainly dominated by contributions from O–H and H–H interactions because of large weightings of $g_{OH}(r)$ and $g_{HH}(r)$, the first two peaks at $r \approx 1.8$ Å and $r \approx 2.4$ Å in $\Delta g^{inter}(r)$, can be assigned to the nearest neighbor hydrogen-bonded O···H and H···H interactions, respectively.

We next perform the least squares fit to the observed $i_X^{inter}(Q)$ (Fig. 7a), in order to determine the structural parameters of the nearest-neighbor intermolecular correlations (r_{ij}, l_{ij}, and n_{ij}). In the fitting procedure, the short-range contributions from O···O, P···O, and P···P interactions, respectively, and the long-range one due to the random distribution of atoms, were taken into account using Eq. 9. The fit was made in the range $1.0 \leq Q \leq 15.0$ Å^{-1}, assuming that statistical errors are uniformly distributed. The calculated $i_X^{inter}(Q)$ and $g_X^{inter}(r)$ are compared with the corresponding observed ones in Figs. 7a and 8a, respectively. A satisfactory agreement is obtained between the calculated and observed $i_X^{inter}(Q)$ over the Q-range covered in the fit. Structural features appearing at $r < 5$ Å in the observed $g_X^{inter}(r)$ are well reproduced by the calculated one. The final values of all independent parameters are summarized in Table 3. The value of the nearest-neighbor hydrogen-bonded O···O distance, $r_{OO} = 2.73(2)$ Å, is ca. 0.1 Å shorter than that reported for liquid pure water,[25,33–38] indicating that a strong hydrogen-bonded network is formed in the concentrated aqueous phosphoric acid solution. The extremely short O···O distance, 2.51(1) Å, which has already been reported based on a previous neutron diffraction study for pure liquid H_3PO_4,[4] reflects the nearest-neighbor hydrogen bonds among H_3PO_4 molecules. The present value of the O···O distance can be regarded as the average value of all hydrogen-bonded O···O distances between H_3PO_4 and H_2O, between H_3PO_4 and H_3PO_4, and between H_2O and H_2O molecules. The nearest-neighbor intermolecular P···O distance, 3.57(1) Å, in the present work agrees well with that found for liquid pure phosphoric acid (3.7(1) Å)[4] and values reported for more dilute aqueous phosphoric acid solutions (3.60—3.73 Å).[5] The second nearest-neighbor O···O_2 interaction at $r = 3.22(1)$ Å, may be attributed to a weakly- or non-hydrogen bonded O···O interaction, which has been reported in pure water[37] and in concentrated aqueous solutions.[39] The present value of the nearest-neighbor P···P distance, 3.63(2) Å, is ca. 0.4 Å shorter than that observed in pure H_3PO_4 crystal (r(P···P) = 4.0 Å)[1] in which

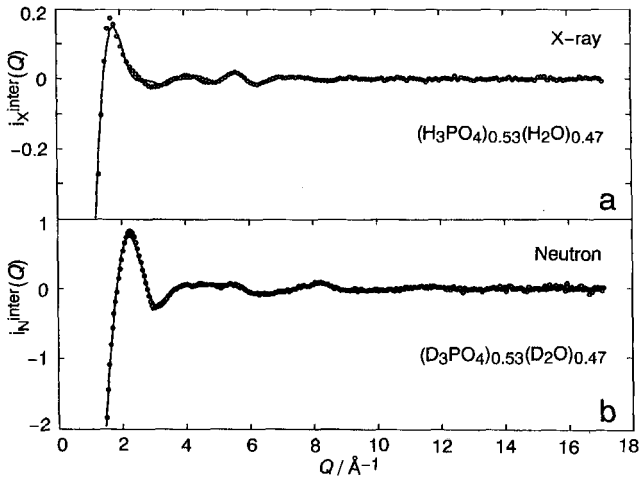

Fig. 7. Observed X-ray and neutron intermolecular interference terms, a) $i_X^{inter}(Q)$ and b) $i_N^{inter}(Q)$, for aqueous 53 mol% phosphoric acid solutions (circles). The best-fit results are indicated by solid lines.

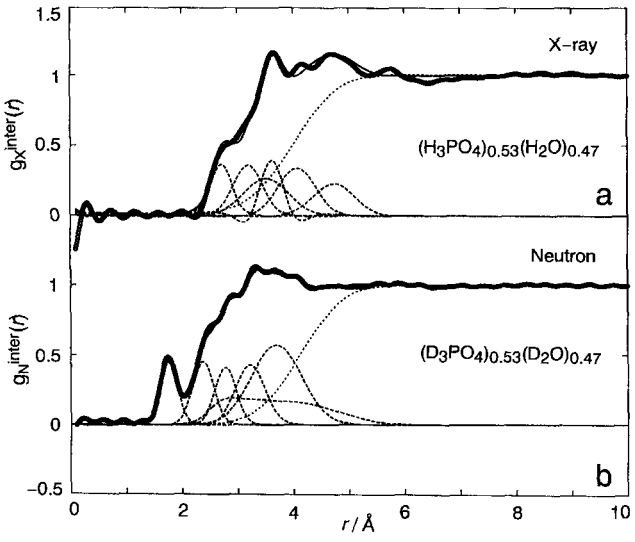

Fig. 8. Observed X-ray and neutron intermolecular distribution functions, a) $g_X^{inter}(r)$ and b) $g_N^{inter}(r)$, for aqueous 53 mol% phosphoric acid solutions (circles). Fourier transform of calculated intermolecular interference terms are indicated by solid lines. Short- and long-range contributions are shown by broken and dotted lines, respectively.

Table 3. Intermolecular Parameters for Aqueous 53 mol% Phosphoric Acid Solutions Determined from the Observed X-Ray Intermolecular Interference Term[a)]

$i\cdots j$	r_{ij}/Å	l_{ij}/Å	n_{ij}
O···O_1	2.73(2)	0.18(1)	1.6(1)
O···O_2	3.22(1)	0.25(2)	2.8(2)
P···O	3.57(1)	0.42(1)	5.2(5)
P···P	3.63(2)	0.22(1)	3.6(2)
O···O_3	4.10(1)	0.32(2)	5.5(2)
O···O_4	4.77(2)	0.36(2)	5.5(5)
	r_{0ij}/Å	l_{0ij}/Å	
Long range	4.11(1)	0.63(1)	

a) Estimated standard deviations are given in parentheses.

Table 4. Intermolecular Parameters for Aqueous 53 mol% Phosphoric Acid Solutions Determined from the Observed Neutron Intermolecular Interference Term[a)]

$i\cdots j$	r_{ij}/Å	l_{ij}/Å	n_{ij}
O···D_1	1.77(1)	0.16(1)	0.71(2)
D···D	2.39(1)	0.19(1)	2.7(1)
P···D	2.75(2)	0.19(2)	8(2)
O···D_2	3.21(2)	0.27(9)	3.8(3)
O···D_3	3.75(8)	0.45(2)	11.4(4)
	r_{0ij}/Å	l_{0ij}/Å	
Long range	4.21(1)	0.62(1)	

a) Estimated standard deviations are given in parentheses.

each H_3PO_4 molecule is connected by two hydrogen bonds. In the present concentrated aqueous H_3PO_4 solution, hydrogen bonds among H_3PO_4 molecules are replaced by hydrogen bonds between H_3PO_4 and H_2O molecules, which may lead to a substantial deformation of a regular array of the hydrogen-bonded H_3PO_4 network. The O···O_3 interaction may be assigned to the non-bonded O···O interaction between neighboring PO_4 units. The present value of the O···O_4 distance, 4.77(2) Å, can be interpreted as the distance of the second nearest-neighbor hydrogen-bonded interaction, such as the O···O···O type.

A least-squares fit for the observed $i_N^{inter}(Q)$ (Fig. 7b) was then performed in the range $1.0 \leq Q \leq 15.0$ Å^{-1}. In the fitting procedure, short-range structural parameters for O···O, P···O, and P···P interactions were fixed at values determined from the X-ray diffraction data mentioned above. A satisfactory agreement is obtained between the calculated and observed $i_N^{inter}(Q)$, as shown in Fig. 7b. The calculated and observed $g_N^{inter}(r)$ are compared in Fig. 8b. Structural features at $r < 4$ Å in the observed $g_N^{inter}(r)$ are well reproduced by the calculated one. The final results of the least-squares fit are listed in Table 4. The nearest-neighbor hydrogen-bonded O···D distance is determined to be 1.77(1) Å, the value of which corresponds to the linear hydrogen bond. The present value of r(O···D) is ca. 0.1 Å shorter than that reported for pure liquid water,[35,40] indicating that a strong hydrogen bond is present in the concentrated aqueous phosphoric acid solution. Since the intermolecular hydrogen-bonded O···D(H) distance, 1.54(1) Å, reported for liquid pure phosphoric acid is much shorter than the present one in the concentrated aqueous phosphoric acid solution, it may be considered that the hydrogen-bonded network structure in the pure phosphoric acid is considerably modified by water molecules. Intermolecular distances for the nearest neighbor D···D and P···D interactions in the present phosphoric acid solution are determined to be 2.39(1) Å and 2.75(2) Å, respectively.

The authors would like to thank Professors Toshiharu Fukunaga (Kyoto University) and Masakatsu Misawa (Niigata University) for their help during the course of the neutron-diffraction measurement. All calculations were carried out with the S7/7000U computer at the Yamagata University Computing Service Center. This work was partially supported by a Grant-in-Aid for Scientific Research No. 09640657 from the Ministry of Education, Science, Sports and Culture.

References

1 S. Furberg, *Acta Chem. Scand.*, **9**, 1557 (1955).
2 R. H. Blessing, *Acta Crystallogr., Sect, B*, **B44**, 334 (1988).
3 A. D. Mighell, J. P. Smith, and W. E. Brown, *Acta Crystallogr., Sect. B*, **B25**, 776 (1969).
4 R. H. Tromp, S. H. Spieser, and G. W. Neilson, *J. Chem. Phys.*, **110**, 2145 (1999).
5 R. Caminiti, P. Cucca, and D. Atzei, *J. Phys. Chem.*, **89**, 1457 (1985).
6 S. C. Lee and R. Kaplow, *Science*, **169**, 477 (1970).
7 D. L. Weltz, *J. Solution Chem.*, **1**, 489 (1972).
8 H. -G. Lee, Y. Matsumoto, T. Yamaguchi, and H. Ohtaki, *Bull. Chem. Soc. Jpn.*, **56**, 443 (1983).
9 R. Triolo and A. H. Narten, *J. Chem. Phys.*, **63**, 3624 (1975).
10 Y. Kameda, T. Usuki, and O. Uemura, *Bull. Chem. Soc. Jpn.*, **71**, 1305 (1998).
11 Y. Kameda, K. Hosoya, S. Sakamoto, H. Suzuki, T. Usuki, and O. Uemura, *J. Mol. Liq.*, **65/66**, 305 (1995).
12 C. Andreani, C. Petrillo, and F. Sacchetti, *Mol. Phys.*, **58**, 299 (1986).
13 C. Andreani and C. Petrillo, *Mol. Phys.*, **62**, 765 (1987).
14 Y. Kameda, H. Ebata, and O. Uemura, *Bull. Chem. Soc. Jpn.*, **67**, 929 (1994).
15 Y. Kameda, I. Sugawara, K. Kijima, T. Usuki, and O. Uemura, *Bull. Chem. Soc. Jpn.*, **68**, 512 (1995).
16 Y. Kameda, R. Takahashi, T. Usuki, and O. Uemura, *Bull. Chem. Soc. Jpn.*, **67**, 956 (1994).
17 T. Fukunaga, M. Misawa, I. Fujikura, and S. Satoh, "KENS Report-IX," (1993), p. 16.
18 G. W. Chantry, "The Raman Effect," ed by A. Anderson, Marcel Dekker Inc., New York (1971), Vol. 1, p. 70.
19 J. R. Scherer, M. K. Go, and S. Kint, *J. Phys. Chem.*, **78**, 1304 (1974).
20 M. Lucas, A. De Trobriand, and M. Ceccaldi, *J. Phys. Chem.*, **79**, 913 (1975).
21 G. E. Walrafen, M. R. Fisher, M. S. Hokmabadi, and W. -H. Young, *J. Chem. Phys.*, **85**, 6970 (1986).
22 "Kagaku Binran," 3rd ed, Maruzen, Tokyo (1984), Vol. II, p. II-338.
23 T. Nakagawa and Y. Oyanagi, "Recent Development in Statistical Inference and Data Analysis," ed by K. Matushita, North-Holland (1980), p. 221.
24 Y. Kameda and O. Uemura, *Bull. Chem. Soc. Jpn.*, **65**, 2021 (1992).
25 A. H. Narten, M. D. Danford, and H. A. Levy, *Disccus. Faraday Soc.*, **43**, 97 (1967).
26 R. Caminiti, P. Cucca, M. Monduzzi, G. Saba, and G. Crisponi, *J. Chem. Phys.*, **81**, 543 (1984).
27 H. Ohtaki and N. Fukushima, *J. Solution Chem.*, **21**, 23 (1992).
28 H. H. Paalman and C. J. Pings, *J. Appl. Phys.*, **33**, 2635 (1962).
29 I. A. Bach and B. L. Averbach, *Phys. Rev.*, **137**, A1113 (1965).
30 T. J. Hanwick and P. Hoffmann, *J. Chem. Phys.*, **17**, 1166 (1949).
31 A. C. Chapman and L. E. Thirlwell, *Spectrochim. Acta*, **20**,

937 (1964).
32 S. Ikawa and M. Kimura, *Bull. Chem. Soc., Jpn.*, **49**, 2051 (1976).
33 F. Hajdu, S. Lengyel, and G. Pálinkás, *J. Appl. Crystallogr.*, **9**, 134 (1976).
34 G. A. Gaballa and G. W. Neilson, *Mol. Phys.*, **50**, 97 (1983).
35 A. K. Soper and M. G. Phillips, *Chem. Phys.*, **107**, 47 (1986).
36 R. Corban and M. D. Zeidler, *Ber. Bunsenges. Phys. Chem.*, **96**, 1463 (1992).
37 K. Yamanaka, T. Yamaguchi, and H. Wakita, *J. Chem. Phys.*, **101**, 9830 (1994).
38 T. Radnai and H. Ohtaki, *Mol. Phys.*, **87**, 103 (1996).
39 Y. Kameda, K. Sugawara, T. Usuki, and O. Uemura, *Bull. Chem. Soc. Jpn.*, **71**, 2769 (1998).
40 A. K. Soper, F. Bruni, and M. A. Ricci, *J. Chem. Phys.*, **106**, 247 (1997).